Talanta 87 (2011) 106–112

Contents lists available at SciVerse ScienceDirect

Talanta

journal homepage: www.elsevier.com/locate/talanta

Application of chitosan/Fe_3O_4 microsphere–graphene composite modified carbon ionic liquid electrode for the electrochemical detection of the PCR product of soybean *Lectin* gene sequence

Wei Sun [a,*], Xiaowei Qi [a], Ying Chen [b], Shengyun Liu [a], Hongwei Gao [c]

[a] *Key Lab of Eco-chemical Engineering of Ministry of Education, College of Chemistry and Molecular Engineering, Qingdao University of Science and Technology, Qingdao 266042, China*
[b] *Institute of Food Safety, Chinese Academy of Inspection and Quarantine, No 3, Road Gao beidian, Beijing, China*
[c] *Shandong Entry-Exit Inspection and Quarantine Bureau of the People's Republic of China, No 70, Road Qutangxia,Qingdao, China*

ARTICLE INFO

Article history:
Received 9 June 2011
Received in revised form
12 September 2011
Accepted 15 September 2011
Available online 1 October 2011

Keywords:
Fe_3O_4 microsphere
Graphene
Chitosan
Carbon ionic liquid electrode
Electrochemical DNA biosensor

ABSTRACT

In this paper a Fe_3O_4 microsphere, graphene (GR) and chitosan (CTS) nanocomposite material modified carbon ionic liquid electrode (CILE) was used as the platform for the construction of a new electrochemical DNA biosensor. The single-stranded DNA (ssDNA) probe was immobilized directly on the surface of the CTS/Fe_3O_4–GR/CILE, which could hybridize with the target ssDNA sequence at the selected conditions. By using methylene blue (MB) as the electrochemical indicator the hybridization reaction was investigated with the reduction peak current measured. By combining the specific properties such as the biocompatibility and big surface area of Fe_3O_4 microspheres, the excellent electron transfer ability of GR, the good film-forming ability of CTS and the high conductivity of CILE, the synergistic effects of nanocomposite increased the amounts of ssDNA adsorbed on the electrode surface and then resulted in the greatly increase of the electrochemical responses. Under the optimal conditions differential pulse voltammetric responses of MB were proportional to the specific ssDNA sequences concentration in the range from 1.0×10^{-12} to 1.0×10^{-6} mol/L with the detection limit as 3.59×10^{-13} mol/L (3σ). This DNA biosensor showed good stability and discrimination ability to one-base and three-base mismatched ssDNA sequences. The polymerase chain reaction (PCR) product of soybean *Lectin* gene sequence was detected by the proposed method with satisfactory result, suggesting that the CTS/Fe_3O_4–GR/CILE was a suitable sensing platform for the sensitive detection of specific gene sequence.

1. Introduction

Electrochemical DNA biosensor, which is based on the immobilization of ssDNA on the electrode surface, has been widely investigated and applied in different fields of the gene detection with the advantages such as high sensitivity, simplicity, low cost, small dimension and cheap instruments [1]. The performances of the electrochemical DNA sensor can be greatly influenced by the ssDNA immobilization methods such as covalent binding, adsorption and polymerization. In recent years, various kinds of nanoparticles have been utilized for the ssDNA probe immobilization due to their unique characteristics such as high surface area, excellent biocompatibility and strong adsorption ability [2]. For example Selvaraju et al. [3] fabricated a sandwich-type electrochemical DNA biosensor using streptavidin-coated magnetic beads and gold nanoparticles as the response magnifiers. The advances in the development of gold nanoparticles based electrochemical DNA biosensors were described in Pingarrón's review [4].

Graphene (GR) is a sheet of sp^2 bonded two-dimensional carbon atoms that are arranged into a honeycomb structure, which has attracted considerable attentions due to its unique and excellent properties, such as extremely high thermal conductivity, good mechanical strength, high mobility of charge carriers, high specific surface area, quantum hall effect and upstanding electric conductivity [5–7]. GR and its based composite materials had been widely used in the fields of electrochemistry and electroanalytical chemistry such as photovoltaic devices, lithium-ion batteries, electrochemical sensors and chemically modified electrodes. Due to the advantages such as wide potential windows, relatively inert electrochemistry and excellent electrocatalytic activities, GR based electrochemical sensors and nano-devices had been applied to the investigation on the DNA hybridization, protein electrochemistry and small electroactive molecules detection. GR also can be used efficiently as a conducting surface with a very high surface area for the deposition of different nanoparticles and consequent electrochemical sensing. For instance, Lim et al. [8] applied the epitaxial

* Corresponding author. Tel.: +86 532 840223927; fax: +86 532 840223927.
E-mail address: sunwei@qust.edu.cn (W. Sun).

0039-9140/$ – see front matter © 2011 Elsevier B.V. All rights reserved.
doi:10.1016/j.talanta.2011.09.047

GR as an anode material for the simultaneous detection of all four DNA bases in double-stranded DNA (dsDNA) without a prehydrolysis step. Yang et al. [9] fabricated a GR-vaseline film modified glassy carbon electrode, which exhibited a good electrochemical activity and stability for fundamental studies on carbon-based electrochemistry. Li's group proved that GR possessed excellent electrocatalytic property towards the oxidation of dopamine and methanol [10,11]. In addition, GR can provide a favorable microenvironment for DNA and effectively accelerate the direct electron transfer rate of DNA at the electrode surface [12,13], which can be further applied to determine DNA with excellent sensitivity.

Magnetite (Fe_3O_4), which has a different valence state, has emerged as a promising supercapacitor material due to its low cost and environmentally benign nature [14]. Wu et al. [15] reported on the capacitive characteristics of nanostructured Fe_3O_4 as an electrode material with a pseudo-capacitance of 27 F/(g-Fe_3O_4). In addition, Fe_3O_4 magnetic nanoparticles (nano-Fe_3O_4) have also attracted an increasing interest in biotechnology and medicine [16]. Due to their properties such as good biocompatibility, strong superparamagnetic property, low toxicity, easy preparation and high adsorption ability, nano-Fe_3O_4 had been used as the modified material in biosensors [17]. Wei et al. [18] developed a dumbbell-like Au-Fe_3O_4 nanoparticles labeled electrochemical immunosensor for the detection of cancer biomarker prostate specific antigen. Tran et al. [19] detected the short HIV sequence with a chitosan/Fe_3O_4 modified screen printed electrode by using MB as redox indicator. Yang et al. [20] fabricated a glucose biosensor by using the intrinsic peroxidase-like activity of Fe_3O_4 nanoparticles in Nafion film with remarkably enhanced sensitivity and selectivity.

Ionic liquids (ILs), which are composed of organic cations and various anions, have been widely used in the fields of chemistry due to the unique advantages such as high chemical and thermal stability, negligible vapor pressure, high ionic conductivity, wide electrochemical windows, low toxicity and the ability to dissolve a wide range of organic and inorganic compounds [21]. Wei and Ivaska [22] reviewed the application of ILs in the electrochemical sensor. ILs can be used as not only the supporting electrolyte but also the modifier in chemically modified electrode. Safavi et al. [23] utilized octylpyridinium hexafluorophosphate as the binder to make a carbon ionic liquid electrode (CILE) for the electrochemical detection. CILE had showed the advantages including high electronic conductivity, remarkable electrocatalytic activity, inexpensive reagents and easily fabrication. Sun et al. applied the CILE as the basal electrode for the redox protein electrochemistry with different nanoparticles such as $CaCO_3$ nanoparticles [24] and CdS nanorods [25].

In this paper, a CILE was fabricated by the addition of 1-butylpyridinium hexafluorophosphate ($BPPF_6$) in carbon paste as binder and modifier, and further used as the basal electrode for the electrochemical DNA biosensor. Then Fe_3O_4 microspheres and GR were mixed together to form a novel nanocomposite material, which was casted on the surface of CILE. Chitosan (CTS) was further dropped on the electrode surface to form a stable film, which could fix the materials tightly on the electrode surface. To the best of our knowledge, the usage of CTS/Fe_3O_4–GR nanocomposite matrix as the DNA immobilization platform for the enlargement of the electrochemical signal of the DNA indicator has not been reported previously. The use of CTS in the composite material can increase the stability of the modifier on the electrode surface. At the same time the Fe_3O_4–GR nanocomposites in the CTS can form a porous structure to provide a specific loading interface for the ssDNA probe immobilization. By combining the advantages of the materials used and with the fabricated CTS/Fe_3O_4–GR/CILE as the basal electrode, ssDNA probe was successfully adsorbed on the modified electrode to get a new electrochemical DNA biosensor, which was applied to the detection of *Lectin* gene sequence fragment of soybean and further used to the polymerase chain reaction (PCR) product of soybean endogenous gene. The proposed DNA biosensor showed the advantages such as the simple preparation procedure, high selectivity and broad linear range.

2. Experimental

2.1. Apparatus and chemicals

All the voltammetric measurements were performed on a CHI 1210A electrochemical workstation (Shanghai CH Instrument, China). Electrochemical impedance spectroscopy (EIS) was performed on a CHI 750B electrochemical workstation (Shanghai CH Instrument, China). A three-electrode system was employed for the electrochemical detection, which was composed of a modified CILE as working electrode, a Pt wire as auxiliary electrode and a saturated calomel electrode (SCE) as reference electrode. Scanning electron microscopy (SEM) was obtained on a JSM-6700F scanning electron microscope (Japan Electron Company, Japan). Nitrogen sorption isotherms were measured with a BelSorp-Mini analyzer (BEL Japan, Inc.) at liquid nitrogen temperature by using a BJH (Barrett–Joyner–Halenda) models for porosity evaluation. The PCR amplification experiments were performed on an Eppendorf Mastercycler Gradient PCR system (Eppendorf, Germany).

1-Butylpyridinium hexafluorophosphate ($BPPF_6$, >99%, Lanzhou Greenchem ILS, LICP, CAS, China), chitosan (CTS, minimum 92% deacetylated, Dalian Xindie Co. Ltd., China), graphite powder (average particle size 30 μm, Shanghai Colloid Chemical Co. Ltd., China), methylene blue (MB, Shanghai Chemicals Plant, China) were used as received. Graphene (GR) was synthesized by the modified Hummer's method [26,27]. Fe_3O_4 microsphere was synthesized by the solvothermal reduction method [28]. Different kinds of buffers such as 10× reaction buffer B (Promega, Wisconsin, USA), Taq DNA polymerase (Promega, Wisconsin, USA), 1× TAE buffer (40.0 mmol/L Tris, 1.0 mmol/L EDTA, 40.0 mmol/L acetate, pH 8.0), 50.0 mmol/L Tris–HCl buffer solution (pH 7.4), 50.0 mmol/L phosphate buffer solution (PBS, pH 7.0) were used and all the solutions were prepared with doubly distilled water.

The 21-base oligonucleotides probe sequences (probe ssDNA), its target complementary sequence DNA (target ssDNA), one-base mismatched ssDNA, three-base mismatched ssDNA and noncomplementary sequence DNA (ncDNA) were synthesized by Shanghai Sangon Biological Engineering Technological Co. Ltd. (China), which were related to the *Lectin* gene sequence of soybean. Their base sequences were listed as below:

- probe ssDNA: 5′-GAA GCT GGC AAC GCT ACC GGT-3′;
- target ssDNA: 5′-ACC GGT AGC GTT GCC AGC TTC-3′;
- one-base mismatched ssDNA: 5′-ACA GGT AGC GTT GCC AGC TTC-3′;
- three-base mismatched ssDNA: 5′-ACA GGT AGC ATT GCC ATC TTC-3′;
- ncDNA: 5′-ACT ACA GCG TTA CGA CTT GTA C-3′.

The DNA samples for PCR amplification were extracted from soybean oil and arachis oil. The PCR reaction was performed on an Eppendorf Mastercycler Gradient PCR system using oligonucleotide primers for *Lectin* gene of soybean with the following sequences:

- Primer F: 5′-GCC CTC TAC TCC ACC CCC ATC C-3′;
- Primer R: 5′-GCC CAT CTG CAA GCC TTT TTG TG-3′.

Arabinose operon D gene of arachis was with the following sequences:

- Primer F: 5′-GCA ACA GGA GCA ACA GTT CAA G-3′;
- Primer R: 5′-CGC TGT GGT GCC CTA AGG-3′.

2.2. Preparation of the modified electrode

Carbon ionic liquid electrode (CILE) was fabricated based on the reported procedure [29]. 3.0 g of graphite powder and 1.0 g of $BPPF_6$ were mixed thoroughly in a mortar and further heated at 80 °C to form a homogeneous carbon paste. A portion of the carbon paste was filled into one end of a glass tube (Φ = 4 mm) and a copper wire was inserted through the opposite end to establish an electrical contact. The CILE surface was smoothed on a piece of weighing paper just before use.

The mixture solution of 1.0 mg/mL Fe_3O_4 microspheres and 1.0 mg/mL GR were prepared in ethanol and sonicated for 0.5 h. Then 3.0 μL of the prepared solution was casted onto the CILE surface. After dried in air at room temperature, 5.0 μL of 1.0 mg/mL CTS (in 1.0% HAc solution) was further coated on the electrode surface and dried to get the modified electrode, which was denoted as CTS/Fe_3O_4–GR/CILE. CTS has been widely used in the electrochemical DNA biosensor as the matrix for the ssDNA immobilization, which can easily interact with DNA and other polyanions through electrostatic attraction [30].

2.3. Fabrication of electrochemical DNA biosensor

The immobilization of probe ssDNA was performed by dropping 10.0 μL of 1.0×10^{-6} mol/L probe ssDNA (in 50.0 mmol/L PBS, pH 7.0) onto the surface of CTS/Fe_3O_4–GR/CILE and dried in air at room temperature. Then the electrode surface was washed with 0.5% sodium dodecyl sulfate (SDS) solution and doubly distilled water for 3 times respectively to remove unabsorbed probe ssDNA on the electrode surface, and the resulted electrode was denoted as ssDNA/CTS/Fe_3O_4–GR/CILE.

The efficient drop hybridization procedure was selected for the DNA hybridization [31,32], which was performed by dropping 5.0 μL target ssDNA (in 50.0 mmol/L PBS) directly onto the surface of ssDNA/CTS/Fe_3O_4–GR/CILE. The hybridization between the target sequence and the probe sequence was allowed to proceed for 10 min at room temperature, and then the electrode was washed with 0.5% SDS solution and doubly distilled water for 3 times successively, to remove the unhybridized target ssDNA. This hybridized electrode was further named as dsDNA/CTS/Fe_3O_4–GR/CILE.

2.4. Electrochemical detection

After hybridization the dsDNA/CTS/Fe_3O_4–GR/CILE was immersed into 4.0×10^{-5} mol/L MB solution for 10 min, then washed with 50.0 mmol/L PBS for 3 times. The cathodic response of the accumulated MB was measured by differential pulse voltammetry (DPV) in a 50.0 mmol/L Tris–HCl buffer solution (containing 20.0 mmol/L NaCl, pH 7.4) with instrumental parameters as: pulse amplitude 0.008 V, pulse width 0.05 s and pulse period 0.2 s.

Cyclic voltammetric experiments were performed in a mixture solution containing 1.0 mmol/L $K_3[Fe(CN)_6]$ and 0.5 mol/L KCl with the scan rate as 100 mV/s. Electrochemical impedance spectroscopy (EIS) was carried out in 1.0 mmol/L $[Fe(CN)_6]^{3-/4-}$ solution containing 0.1 mol/L KCl with the frequencies swept from 10^4 to 1.0 Hz.

2.5. Polymerase chain reaction of soybean endogenous genes sequence

The amplification of *Lectin* gene fragments was performed in a final volume of 25 μL in 0.2 mL tube, which contained 200.0 nmol/L each primer of *Lectin* primer F and *Lectin* primer R, 10× reaction buffer B (Promega, Wisconsin, USA), 2.0 mmol/L $MgCl_2$, 200.0 nmol/L of dATP, dCTP, dGTP and dTTP, 1.5 units of Taq DNA polymerase (Promega, Wisconsin, USA) and 1.0 μL DNA template purified from samples.

In the PCR experiments, DNA was first denatured at 94 °C for 30 s. Then PCR was carried out with the following experimental conditions: 35 cycles of amplification (94 °C for 30 s, 56 °C for 30 s, 72 °C for 30 s) and final extension at 72 °C for 5 min. The PCR products were analyzed by electrophoresis separation at 5 V/cm for 40 min on a 2% agarose gel that contained 0.5 μg/mL ethidium bromide in 1× TAE buffer (40.0 mmol/L Tris, 1.0 mmol/L EDTA, 40.0 mmol/L acetate, pH 8.0), and finally visualized with a UV transilluminator. The PCR products of *Lectin* gene were kept at 4 °C before use. The amplification of arachis *Arabinose operon D* gene fragments was also performed by the similar procedure.

3. Results and discussion

3.1. Morphology of the Fe_3O_4–GR composite

The SEM images of nanomaterials used were recorded with the results shown in Fig. 1. In Fig. 1A ball-like nanostructures Fe_3O_4 mesoporous sphere appeared with the width in the range of 100–200 nm. Fig. 1B showed the typical ultrathin sheets and wrinkles of GR. This wrinkled nature of GR is highly beneficial in maintaining a high surface area on the electrode since the sheets cannot readily collapse back to a graphitic structure. The high surface area is helpful in increasing the surface loading of probe ssDNA on the surface. The excellent conductivity and small band gap of GR are favorable for conducting electrons from the biomolecules [12]. By mixing Fe_3O_4 microspheres and GR together in ethanol and sonicated for 15 min, the image of Fe_3O_4–GR nanocomposite was shown in Fig. 1C. It can be seen that the Fe_3O_4 microspheres were well-distributed and surrounded by wrinkled flake-like GR, which could provide an increased roughness of the electrode surface.

The nitrogen adsorption/desorption isotherms were carried out to investigate the porosity of Fe_3O_4 microspheres and Fe_3O_4–GR nanocomposite. As shown in Fig. 2A, the nitrogen adsorption and desorption isotherms of Fe_3O_4 microspheres exhibited the characteristic of a type III isotherm with a type H3 hysteresis loop, indicating the presence of mesopores with the size range from 5 to 50 nm (insert of Fig. 2A) [33]. In addition, the observed hysteresis loop shifted to a higher relative pressure with the p/p_0 value to 1, indicated that macropores (size >50 nm) were also present. It can be observed that the sizes of mesopores centralize on two areas with the peak values as 10.6 and 29.8 nm, respectively. The nitrogen adsorption/desorption of Fe_3O_4–GR nanocomposite was also investigated with the result shown in Fig. 2B. Due to the presence of GR nanosheet in the composite, a much better porosity appeared with the size of mesopores centralized at 1.9 nm, 10.6 nm and 25.8 nm, respectively, which indicated that the interaction of Fe_3O_4 microsphere and GR nanosheet resulted in the formation of composite with many micropores. So the roughness of the electrode surface was increased and more ssDNA could be adsorbed on the pore site of the composite.

3.2. Electrochemical characteristics of the modified electrodes

Cyclic voltammograms of different modified electrodes in a 1.0 mmol/L $[Fe(CN)_6]^{3-}$ solution were shown in Fig. 3A. On CILE a couple of well-defined redox peaks was observed (curve a), which was due to the high ionic conductivity of IL present in the carbon paste. On the CTS/Fe_3O_4/CILE an increased electrochemical response of potassium ferricyanide was observed (curve b), which could be attributed to the presence of Fe_3O_4 microspheres

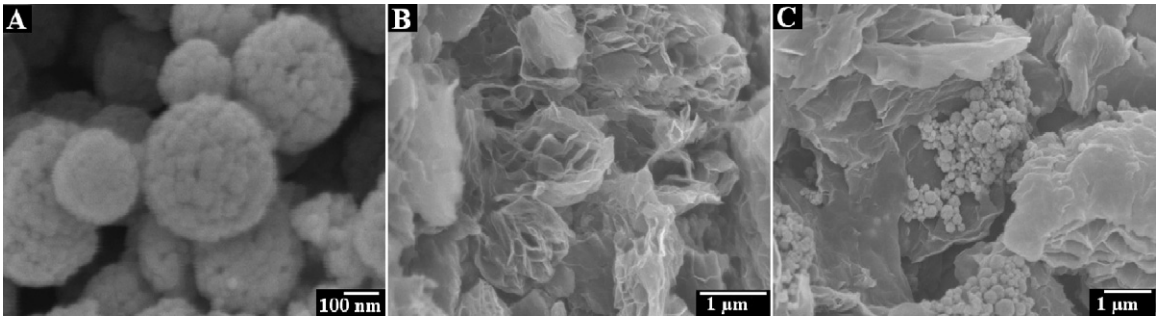

Fig. 1. SEM images of Fe_3O_4 microsphere (A), GR (B) and Fe_3O_4–GR mixture (C).

on the electrode surface. On the CTS/GR/CILE the electrochemical response was further increased (curve c), indicating the presence of GR greatly improved the electrode performance. GR had been elucidated to have the advantages such as big surface area, small band gap, excellent electrical conductivity, high electron mobility and low electronic noise from thermal effect at room temperature [12]. So the presence of GR on the electrode surface can accelerate the electron transfer rate between the redox couple in bulk solution and the electrode. On the CTS/Fe_3O_4–GR/CILE the redox peak currents were further increased (curve d), which could be attributed to the synergistic amplification effects of Fe_3O_4 microsphere and GR in the composite film. The Fe_3O_4–GR nanocomposite can effectively improve the electrochemical reaction rate of the redox probe. According to the Randles–Sevcik equation [34]:

$$I_{pc} = (2.69 \times 10^5) n^{3/2} A D^{1/2} C^* \nu^{1/2}$$

where I_{pc} is the reduction peak current (A), n is the electron transfer number, A is the apparent electrode area (cm^2), D is the diffusion coefficient of $K_3[Fe(CN)_6]$ in the solution (cm^2/s), C^* is the concentration of $K_3[Fe(CN)_6]$ (mol/cm^3) and ν is the scan rate (V/s), the apparent electroactive area of different electrodes can be calculated. By exploring the reduction peak current with scan rate, the average apparent electrode area of CILE, CTS/Fe_3O_4/CILE, CTS/GR/CILE and CTS/Fe_3O_4–GR/CILE were calculated as 0.170 cm^2, 0.426 cm^2, 0.538 cm^2 and 0.578 cm^2, respectively. The results indicated that the presence of Fe_3O_4 microspheres and GR in the CTS film could greatly improve the apparent electrode area, so the electrochemical responses were gradually enhanced on the modified electrodes. The capacitance of different modified electrodes can be calculated by using the equation of $C^{app} = I/S\nu$ [35], where I is the average of the positive and the negative charging current obtained from the cyclic voltammetric curves at 0.4 V, S is the geometric area of the electrode; ν is the scan rate. By measuring the background current of the electrode in the 0.05 mol/L phosphate buffer solution (pH 7.4), the capacitance value of CILE, CTS/Fe_3O_4/CILE, CTS/GR/CILE and CTS/Fe_3O_4–GR/CILE were calculated as 334.4 μF/cm^2, 628.0 μF/cm^2, 654.4 μF/cm^2, 755.73 μF/cm^2, respectively. The capacitance values increased gradually with the further modification of the composite materials and the results were in good agreement with the increase of the apparent electrode area, which further proved the presence of nanocomposite on the electrode.

The modified electrodes were further characterized by electrochemical impedance spectroscopy (EIS) and the semicircle portion observed at high frequencies in the Nyquist diagrams corresponded to the electron transfer limiting process. The interfacial electron transfer resistance (R_{et}) can be calculated from the diameter of Nyquist diagram, so the Nyquist diagrams of different modified electrodes were recorded. As illustrated in Fig. 3B, the R_{et} value of CILE was got as 51.6 Ω (curve a). On the CTS/Fe_3O_4/CILE and CTS/GR/CILE the R_{et} values decreased to 28.4 Ω (curve b) and 10.1 Ω (curve c), respectively, indicating the presence of Fe_3O_4 microsphere and GR on the electrode surface could obviously increase the conductivity of the electrode surface and decrease the impedance. On the CTS/Fe_3O_4–GR/CILE (curve d) a straight line appeared, indicating the highest conductivity of the electrode interface. So the synergistic effects of Fe_3O_4 and GR in the film greatly decreased the resistance for the electron transfer. The agreement of EIS with cyclic voltammetric results indicated that the CTS/Fe_3O_4–GR composite film was an excellent platform for the electrode modification.

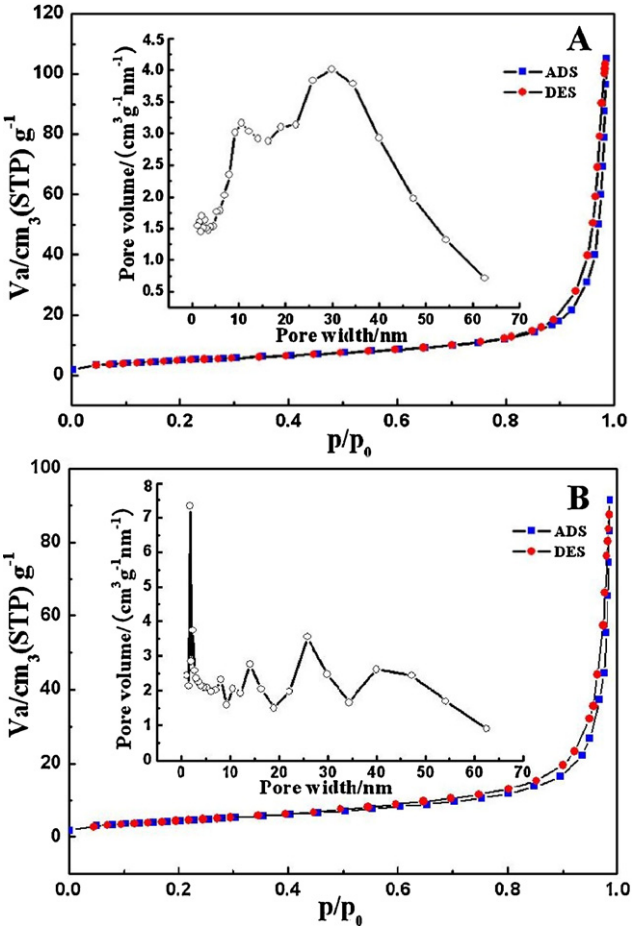

Fig. 2. Nitrogen adsorption (ADS)/desorption (DES) isotherms of Fe_3O_4 microsphere (A) and Fe_3O_4–GR mixture (B). Inset is the corresponding pore size distribution.

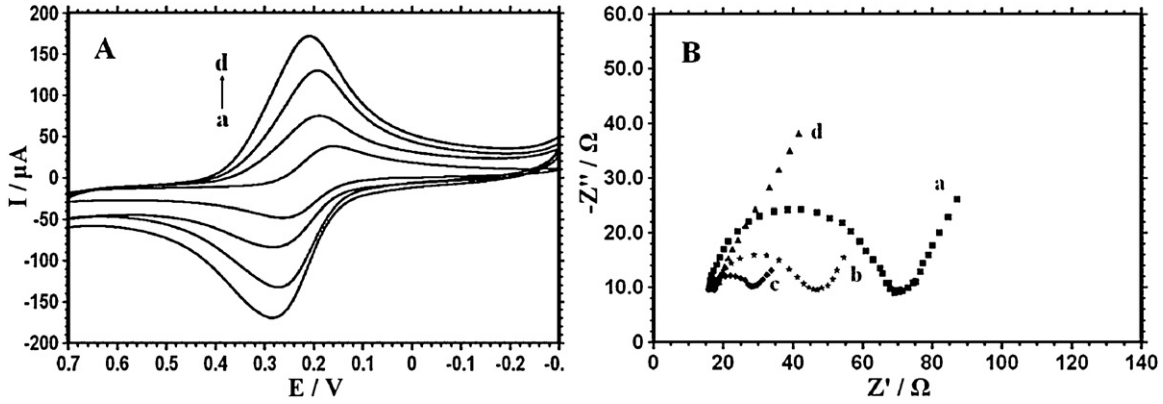

Fig. 3. (A) Cyclic voltammograms of different modified electrodes in a 1.0×10^{-3} mol/L $K_3[Fe(CN)_6]$ and 0.5 mol/L KCl solution with scan rate as 100 mV/s. (B) Electrochemical impedance spectra of different modified electrodes in 1.0 mmol/L $[Fe(CN)_6]^{3-/4-}$ solution containing 0.1 mol/L KCl. From a to d were CILE, CTS/Fe_3O_4/CILE, CTS/GR/CILE and CTS/Fe_3O_4–GR/CILE, respectively.

3.3. Differential pulse voltammograms of MB

MB is often used as the electrochemical indicator in the electrochemical DNA biosensor, which exhibits excellent distinguish ability to ssDNA and dsDNA on the electrode surface due to the different interaction models [36]. Fig. 4 showed the differential pulse voltammograms of MB on dsDNA/CTS/CILE (curve a), dsDNA/CTS/Fe_3O_4/CILE (curve b), dsDNA/CTS/GR/CILE (curve c) and dsDNA/CTS/Fe_3O_4–GR/CILE (curve d) in 50.0 mmol/L Tris–HCl buffer solution. The reduction peak current of MB increased gradually with the step-by-step incorporation of nanomaterials in the film, indicating more dsDNA molecules was present on the electrode surface. The results were attributed to the gradually increase of the apparent electrode area, which could immobilize more dsDNA on the electrode surface. dsDNA can further interact with MB and accumulate more MB molecules on the electrode surface, so the increase of the reduction peak current appeared. The largest reduction peak current appeared on the dsDNA/CTS/Fe_3O_4–GR/CILE, indicating that the biggest adsorption amounts of MB molecules that interacted with dsDNA. The above results confirmed that the synergetic effects of Fe_3O_4 microsphere and GR in the nanocomposite film could effectively enhance the surface concentration of dsDNA due to the large surface area and roughness of the electrode interface.

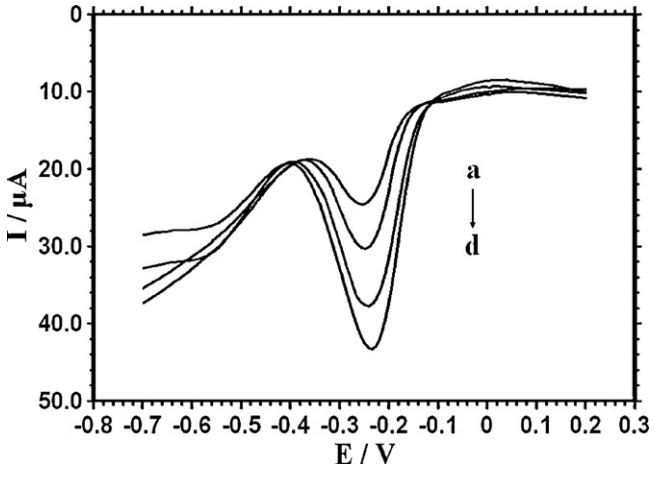

Fig. 4. Differential pulse voltammograms of 4.0×10^{-5} mol/L MB on (a) dsDNA/CTS/CILE, (b) dsDNA/CTS/Fe_3O_4/CILE, (c) dsDNA/CTS/GR/CILE and (d) dsDNA/CTS/Fe_3O_4–GR/CILE in 50 mmol/L Tris–HCl buffer solution contained 20.0 mmol/L NaCl (pH 7.4).

3.4. Optimization of the electrode preparation

The ratio of Fe_3O_4 microspheres and GR in the composite on the electrode surface influenced the electron transfer rate and the maximum loading amount of ssDNA probe on the electrode surface. Different mass ratio of Fe_3O_4 microspheres and GR such as 4:1, 3:2, 1:1, 2:3 and 1:4 was studied with the total mass of Fe_3O_4 microspheres and GR unchanged. When the proportion of Fe_3O_4 was too low (1:4), the immobilization amount of ssDNA probes was limited. When the quantity of poor electrical conductive Fe_3O_4 was too large (4:1), the conductivity of the nanocomposite membrane modified electrode decreased obviously. Therefore, the mixture of 1.0 mg Fe_3O_4 microspheres and 1.0 mg GR dispersed in 1.0 mL ethanol was chosen in the experiments.

CTS is a natural cationic biopolymer with excellent film-forming ability and biocompatibility [37,38], which has been widely used in the electrochemical DNA biosensor for the ssDNA immobilization through electrostatic attraction between the polycationic chitosan oligomer and the polyanionic DNA backbone [30]. Based on the reference [38], a 1.0 mg/mL CTS solution was commonly used for the electrode modification, which was dissolved in a 1.0% HAc solution in this experiment.

According to the reported result [39], the maximum coverage density of ssDNA on the electrode surface was 2.7×10^{12} molecules/cm^2, which was about 4.6×10^{-12} mol/cm^2. Since appropriate surface probe concentration can form a probe monolayer that is benefit to the further hybridization. So 10 μL of the 1.0×10^{-6} mol/L ssDNA probe sequence was dropped on the surface of the modified electrode, which gave a surface concentration of 1.7×10^{-11} mol/cm^2. The excess amount of ssDNA probe sequence on the electrode surface can result in the saturated adsorption of probe, which was beneficial to the following hybridization reaction with the target ssDNA sequence.

3.5. Selectivity of the electrochemical DNA biosensor

The selectivity of this electrochemical DNA biosensor was investigated by using the probe ssDNA modified electrode to hybridize with different ssDNA sequences related to target ssDNA sequence. Fig. 5 showed the DPV reductive responses of MB at the ssDNA probe-modified electrode (curve a) and after hybridization with different kinds of ssDNA sequence. After hybridized with the target ssDNA, the biggest reduction signal was obtained (curve e), indicating the formation of hybridized dsDNA on the electrode surface could accumulate the most amounts of MB molecules. The hybridization with the noncomplementary sequence (curve b) gave

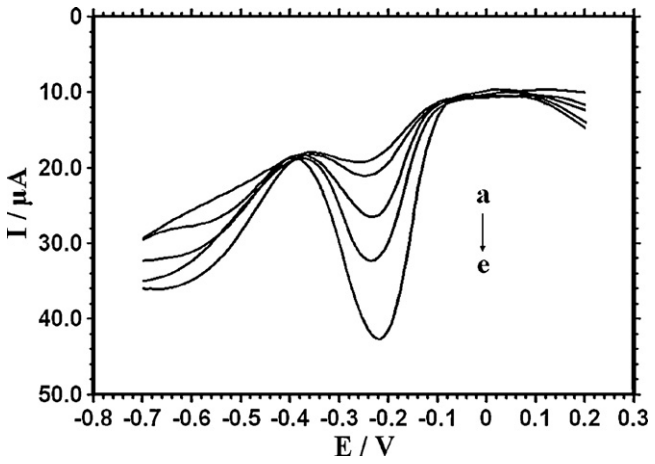

Fig. 5. Differential pulse voltammograms of MB at the ssDNA probe-modified electrode (a) and after hybridization with the noncomplementary sequence (b), three-base mismatched sequence (c), one-base mismatched sequence (d), the complementary DNA sequence (e).

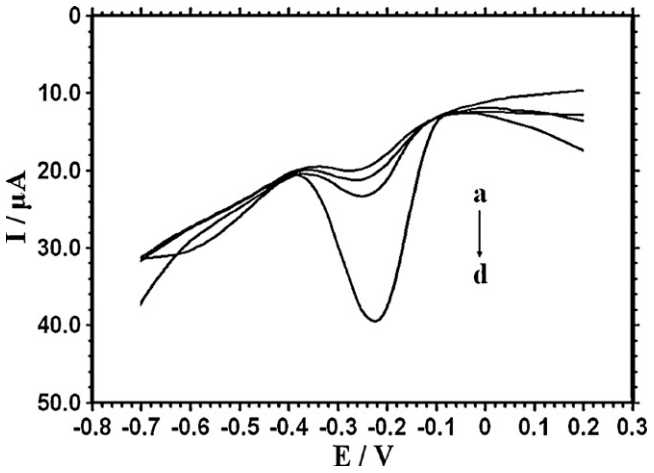

Fig. 6. Differential pulse voltammograms of MB on (a) CTS/Fe_3O_4–GR/CILE, probe/CTS/Fe_3O_4–GR/CILE (b) and hybridization with PCR products of arachis (c) and soybean (d) endogenous genes.

a small increase of the electrochemical response. MB can interact with phosphate framework of ssDNA by electrostatic binding, while the electrostatic effect and intercalation with the major or minor grooves of dsDNA helix are coexisted [36]. The little increase of the peak current can be attributed to the electrostatic interaction of MB with non-specific adsorbed noncomplementary ssDNA on the electrode surface. After the ssDNA probe was hybridized with three-base mismatched sequence (curve c) and one-base mismatched sequence (curve d), the increases of the reductive peak current were much smaller than that obtained from the complementary ssDNA sequence. At the same time the one-base mismatched sequence gave a bigger response than that of the three-base mismatched sequence, which demonstrated that the fabricated DNA biosensor exhibited the high selectivity and good distinguish ability for the hybridization detection.

3.6. Sensitivity of the electrochemical DNA sensor

The sensitivity of this electrochemical DNA biosensor was explored by hybridizing the probe ssDNA modified electrode with the different concentrations of *Lectin* gene sequence of soybean. With the increase of the target ssDNA concentration in the solution the reduction peak current of MB also increased gradually and reached its maximum level at a concentration of 1.0×10^{-6} mol/L. Thus, at this concentration of target ssDNA the maximum capacity of the probe ssDNA available on the electrode surface is involved in the hybridization event. The calibration curve for *Lectin* gene sequence of soybean is linear between 1.0×10^{-12} mol/L and 1.0×10^{-6} mol/L with a correlation coefficient of 0.998 and the linear regression equation of ΔI (μA) = 2.508 log[c/(mol/L)] + 53.014 (where c is the concentration of soybean *Lectin* gene sequence; ΔI is the difference of MB peak current before and after hybridization). The relative standard deviation (RSD) of six independently probe-modified electrodes measured for target ssDNA sequence was 4.3%, indicating the good reproducibility of the detection. A detection limit of the soybean *Lectin* gene sequence was estimated to be 3.59×10^{-13} mol/L (3σ) (where σ is the RSD of the blank solution, $n = 11$). The performance of the proposed biosensor was compared with that of other electrochemical DNA biosensors based on different nanoparticles with the results shown in Table 1. It can be seen that the proposed DNA biosensor had a lower detection limit and wider detection range for the target ssDNA sequence assay.

The stability of ssDNA/CTS/Fe_3O_4–GR/CILE was further investigated by hybridizing with the target sequence after different storage time at 4 °C refrigerator. After 10 days storage of the modified electrode, 97.5% of the initial sensitivity remained. After 20 days storage 95.2% of the initial sensitivity still remained. The results indicated this modified electrode was a stable platform as electrochemical DNA biosensor.

3.7. Detection of PCR product of soybean endogenous genes

The hybridization detection of the PCR amplified real samples of soybean (*Lectin* gene) and arachis (*Arabinose operon D* gene) endogenous gene were further conducted by this electrochemical DNA biosensor under the selected conditions. The PCR amplified samples were diluted with 50.0 mmol/L PBS (pH 7.0) and denatured by heating it in boiling water bath for 10 min, and further frozen in an ice bath for 2 min. Then the denatured PCR amplification product of soybean and arachis endogenous gene samples was dropped directly onto ssDNA/CTS/Fe_3O_4–GR/CILE for hybridization. After the hybridization reaction the electrode was immersed into MB solution for detection with the results shown in Fig. 6. The MB signal at the probe ssDNA modified electrode (curve b) was bigger than that of the CTS/Fe_3O_4–GR/CILE (curve a), indicating that the presence of ssDNA on the electrode surface could

Table 1
Comparison of the analytical parameters with other modified electrodes.

Substrate electrode	Modifier	Detection method	Indicator	Linear range (mol/L)	Detection limit (mol/L)	References
SPE[a]	CTS/Fe_3O_4	SWV	MB	5.0×10^{-11} to 3.0×10^{-10}	5.0×10^{-11}	[19]
GE[b]	CTS/MWCNTs	DPV	MB	5.0×10^{-9} to 2.0×10^{-8}	2.52×10^{-10}	[40]
GCE[c]	MWCNTs/ZrO_2	DPV	Daunomycin	1.49×10^{-10} to 9.32×10^{-8}	7.5×10^{-11}	[41]
CILE	CTS/Fe_3O_4–GR	DPV	MB	1.0×10^{-12} to 1.0×10^{-6}	3.59×10^{-13}	This work

[a] SPE, screen printed electrode.
[b] GE, graphite electrode.
[c] GCE, glassy carbon electrode.

adsorb MB molecules. An increase of the MB reduction peak current appeared after the hybridization with the denatured PCR amplified real sample of *Arabinose operon D* gene (curve c), which was much smaller than hybridized with the denatured PCR amplified real sample of *Lectin* gene (curve d), indicating the good selectivity of this constructed electrochemical DNA biosensor, and the increase on the curve c may be caused by the non-specific adsorption of sample ssDNA. The obvious increase on curve d indicated the successful accomplishment of the hybridization reaction on the electrode surface, which resulted in the formation of dsDNA with more MB accumulated. This significant difference of the MB signals between the probe modified electrode and at the hybridized electrode confirmed that this electrochemical DNA biosensor could effectively detect the PCR product of soybean *Lectin* gene sample.

4. Conclusions

A sensitive electrochemical DNA sensor based on the CTS/Fe_3O_4–GR/CILE was developed and further applied to the detection of the PCR product from soybean *Lectin* gene. The surface of the modified electrodes was characterized by different methods including SEM, cyclic voltammetry and electrochemical impedance spectroscopy. Due to the synergistic effects of Fe_3O_4 microspheres and GR on the electrode surface, the apparent electrode area was increased, which further enhanced the loading amount of the probe ssDNA sequence and improved the detection sensitivity for target ssDNA sequence. This electrochemical DNA sensor exhibited the advantages such as simple preparation procedure, low cost, fast response, good selectivity, wide linear range and high sensitivity. The detection of the soybean *Lectin* gene sequence can be achieved in the concentration range from 1.0×10^{-12} to 1.0×10^{-6} mol/L with the detection limit of 3.59×10^{-13} mol/L (3σ). The PCR product of soybean *Lectin* gene sample was also detected satisfactorily and the method exhibited a well-distinguished ability with that of arachis.

Acknowledgements

We acknowledge the financial supports provided by the National Natural Science Foundation of China (21075071), the project of Chinese Academy of Inspection and Quarantine (Jianke2009jk033), National Department Public Benefit Research Foundation (201110015), 11th Five Years Key Programs for Science and Technology Development of China (2008ZX08012-001) and the Shandong Province Natural Science Foundation (ZR2009BL017).

References

[1] F.R.R. Teles, L.P. Fonseca, Talanta 77 (2008) 606–623.
[2] J. Wang, Anal. Chem. 500 (2003) 247–257.
[3] T. Selvaraju, J. Das, K. Jo, K. Kwon, C. Huh, T.K. Kim, H. Yang, Langmuir 24 (2008) 9883–9888.
[4] J.M. Pingarrón, P.Y. Sedeño, A.G. Cortés, Anal. Bioanal. Chem. 19 (2008) 5848–5866.
[5] A. Novoselov, Nat. Mater. 6 (2007) 183–191.
[6] D. Li, M.B. Müller, S. Gilje, R.B. Kaner, G.G. Wallace, Nat. Nanotechnol. 3 (2008) 101–105.
[7] S. Park, R.S. Ruoff, Nat. Nanotechnol. 4 (2009) 217–224.
[8] C.X. Lim, H.Y. Hoh, P.K. Ang, K.P. Loh, Anal. Chem. 82 (2010) 7387–7393.
[9] S. Yang, D. Guo, L. Su, P. Yu, D. Li, J. Ye, L. Mao, Electrochem. Commun. 11 (2009) 1912–1915.
[10] Y. Wang, Y. Li, L. Tang, J. Lu, J. Li, Electrochem. Commun. 11 (2009) 889–892.
[11] Y. Li, L. Tang, J. Li, Electrochem. Commun. 11 (2009) 846–849.
[12] S. Stankovich, D.A. Dikin, G.H.B. Dommett, K.M. Kohlhaas, E.J. Zimney, E.A. Stach, R.D. Piner, S.T. Nguyen, R.S. Ruoff, Nature 442 (2006) 282–286.
[13] H.W.Ch. Postma, Nano. Lett. 10 (2010) 420–425.
[14] X. Du, C. Wang, M. Chen, Y. Jiao, J. Wang, J. Phys. Chem. C 113 (2009) 2643–2646.
[15] N.L. Wu, S.Y. Wang, C.Y. Han, D.S. Wu, L.R. Shiue, J. Power Sources 113 (2003) 173–178.
[16] D.F. Cao, N.F. Hu, Biophys. Chem. 121 (2006) 209–217.
[17] Y. Cheng, Y. Liu, J. Huang, K. Li, Y. Xian, W. Zhang, L. Jin, Electrochim. Acta 54 (2009) 2588–2594.
[18] Q. Wei, Z. Xiang, J. He, G.L. Wang, H. Li, Z.Y. Qian, M.H. Yang, Biosens. Bioelectron 26 (2010) 627–631.
[19] L.D. Tran, B.H. Nguyen, N.V. Hieu, H.V. Tran, H.L. Nguyen, P.X. Nguyen, Mater. Sci. Eng. C 31 (2011) 477–485.
[20] L.Q. Yang, X.L. Ren, F.Q. Tang, L. Zhang, Biosens. Bioelectron 25 (2009) 889–895.
[21] S. Pandey, Anal. Chim. Acta 556 (2006) 38–45.
[22] D. Wei, A. Ivaska, Anal. Chim. Acta 607 (2008) 126–135.
[23] A. Safavi, N. Maleki, O. Moradlou, M. Sorouri, Electrochem. Commun. 10 (2008) 420–423.
[24] W. Sun, R.F. Gao, K. Jiao, J. Phys. Chem. B 111 (2007) 4560–4567.
[25] W. Sun, D.D. Wang, K. Jiao, Electrochim. Acta 53 (2008) 8217–8221.
[26] W.S. Hummers Jr., R.E. Offeman, J. Am. Chem. Soc. 80 (1958) 1339.
[27] N.I. Kovtyukhova, P.J. Ollivier, B.R. Martin, T.E. Mallouk, S.A. Chizhik, E.V. Buzaneva, A.D. Gorchinskiy, Chem. Mater. 11 (1999) 771–778.
[28] H.B. Hu, Z.H. Wang, L. Pan, S.P. Zhao, S.Y. Zhu, J. Phys. Chem. C 114 (2010) 7738–7742.
[29] W. Sun, M.X. Yang, R.F. Gao, K. Jiao, Electroanalysis 19 (2007) 1597–1602.
[30] C. Xu, H. Cai, Q. Xu, P. He, Y. Fang, Fresenius J. Anal. Chem. 369 (2001) 428–432.
[31] M.S. Hejazi, M.H. Pournaghi-Azar, E. Alipour, F. Karimi, Biosens. Bioelectron 23 (2008) 1588–1594.
[32] M.H. Pournaghi-Azar, E. Alipour, S. Zununi, H. Froohandeh, M.S. Hejazi, Biosens. Bioelectron 24 (2008) 524–530.
[33] D.V. Bavykin, V.N. Parmon, A.A. Lapkin, F.C. Walsh, J. Mater. Chem. 14 (2004) 3370–3377.
[34] A.J. Bard, L.R. Faulkner, Electrochemical Methods, 2nd ed., Wiley, New York, 2001, p. 213.
[35] M.D. Anjo, M. Kahr, M.M. Khodabakhsh, S. Nowinski, M. Wagner, Anal. Chem. 61 (1989) 2603–2608.
[36] S.O. Kelley, J.K. Barton, Bioconjugate Chem. 8 (1997) 31–37.
[37] M. Rinaudo, Prog. Polym. Sci. 31 (2006) 603–632.
[38] C.S. Shan, H.F. Yang, D.X. Han, Q.X. Zhang, A. Ivaska, L. Niu, Biosens. Bioelectron 25 (2010) 1504–1508.
[39] V. Chan, D.J. Graves, S.E. McKenzie, Biophys. J. 69 (1995) 2243–2255.
[40] J. Li, Q. Liu, Y.J. Liu, S.C. Liu, S.Z. Yao, Anal. Biochem. 346 (2005) 107–114.
[41] Y.H. Yang, Z.J. Wang, M.H. Yang, J.S. Li, F. Zheng, G.L. Shen, R.Q. Yu, Anal. Chim. Acta 584 (2007) 268–274.